Proceedings of Anticancer Research, 2025, Volume 9, Issue 2
http://ojs.bbwpublisher.com/index.php/PAR
ISSN Online: 2208-3553
ISSN Print: 2208-3545

Antioxidant Protective Effect of Melatonin on Cyclophosphamide-Induced Premature Ovarian Failure and its Mechanism

Chongran Liu, Tongtong Wei, Xinyue Rao, Ziqi Fan, Minghui Hao, Wanjing Wang, Yihang Song*

Medical College, Northwest Minzu University, Lanzhou 730000, Gansu, China

***Corresponding author:** Yihang Song, 284132319@xbmu.edu.cn

Copyright: © 2025 Author(s). This is an open-access article distributed under the terms of the Creative Commons Attribution License (CC BY 4.0), permitting distribution and reproduction in any medium, provided the original work is cited.

Abstract: *Objective:* To study the antioxidant protective effect and mechanism of melatonin on cyclophosphamide-induced premature ovarian failure model mice. *Methods:* Six-month sexually mature female Kunming mice were taken for one week of acclimatization and then randomly divided into a normal group, blank control group, drug control group, ovarian premature aging model group, and melatonin intervention low, medium, and high dose group, with 20 mice in each group. We observed the status and body mass of the mice in each group; observed and monitored the estrous cycle by HE staining; measured the diameter and size of the ovaries and weighed the wet weight of the ovaries; observed the morphological changes of the ovaries by HE staining and counted the developing follicles at all levels; detected the levels of serum estradiol (E2), follicle-stimulating hormone (FSH), and luteinizing hormone (LH) by ELISA; measured the levels of serum MDA, SOD, and GSH-PX by antioxidant kit; detected the levels of protein immunoblotting by ELISA; protein immunoblotting (Western blot) to examine the expression of DNA damage-related proteins γH2AX, p53, and p21 in ovarian tissues. *Results:* Compared with the control group, mice in the premature ovarian failure model group showed reduced mobility, rough hair, decreased body weight, disorganized estrous cycle, decreased ovarian weight ($P < 0.05$), decreased number of follicles at all levels of development ($P < 0.05$), increased number of atretic follicles ($P < 0.05$), significantly elevated levels of serum FSH and LH, significantly decreased levels of E2 ($P < 0.05$), significantly increased levels of serum MDA, significantly lower SOD and GSH-PX levels ($P < 0.05$), and the expression of p53, p21, and γH2AX in ovarian tissues was increased ($P < 0.05$). Compared with the model group of premature ovarian failure, melatonin improved the changes of the above indexes induced by cyclophosphamide-induced premature ovarian failure in mice. *Conclusion:* Melatonin can improve the changes of motility cycle disorders, abnormal follicular development, and abnormal serum hormone levels induced by cyclophosphamide-induced oxidative stress in mice with premature ovarian failure. At the same time, melatonin can improve the oxidative stress induced by cyclophosphamide and alleviate the role of oxidative stress-induced DNA damage in mouse ovaries by exerting its antioxidant effect.

Keywords: Melatonin; Cyclophosphamide; Premature ovarian failure; Antioxidation

Online publication: April 2, 2025

1. Introduction

The global incidence of premature ovarian failure (POF) is approximately 1–7%. In China, the incidence of this disease accounts for about 2.8%, and there is an increasing trend year by year and younger patients being affected [1,2]. POF refers to the amenorrhea phenomenon before the age of 40 caused by the exhaustion of female ovarian function. Clinical manifestations include high follicle-stimulating hormone levels (FSH > 40 U/L with testing periods of over one month), declined estrogen levels (LH < 73.2 pmol/L), perimenopausal symptoms such as strange menstruation (scanty or amenorrhea), hot flashes and anguish, sorrowful mood, concern dozing, doubled incidence of heart disease, and dropped bone mineral density, which are the causes of abnormal reproductive health in women [3]. The occurrence of POF is related to genetics, radiotherapy and chemotherapy treatment, ovarian surgery history, autoimmune dysfunction, and metabolic disorders [4-6]. Among them, chemotherapy-induced POF has become a clinical concern [7]. Cyclophosphamide (CTX), a commonly used chemotherapeutic drug for anti-tumor treatment in clinical practice, belongs to the alkylating agent category. It has the greatest toxic effect on the female reproductive system, especially the ovaries, and exhibits a dose-dependent effect. CTX can promote ovarian granulosa cell death, resulting in an aberrant reduction in the number of ovarian follicles, depletion of ovarian follicular reserves, ovarian dysfunction, and eventually premature ovarian failure [8-10]. Melatonin (MT), an indoleamine hormone secreted by the mammalian hypothalamic pineal gland, is an often utilized free-radical scavenger in clinical practice. It is secreted in a circadian rhythm, reaching a peak at night. According to research, it has been suggested that the concentration of MT in human follicular fluid is higher than that in the blood [11]. Numerous previous studies have confirmed that MT can improve ovarian oxidative stress through its antioxidant capacity, thereby inhibiting ovarian granulosa cell apoptosis, preserving ovarian reserve function, improving fertility, and enhancing pregnancy outcomes [12-14]. This study intends to explore the antioxidant protective effect and molecular mechanism of MT on CTX-induced premature ovarian failure by using MT on a CTX-induced premature ovarian failure mouse model. It is hoped that this will provide a basic theoretical foundation and new ideas for clinical preventive treatment of chemotherapy-induced premature ovarian failure.

2. Materials and methods

2.1. Materials

2.1.1. Experimental animals and environment

A total of 140 sexually mature female Kunming mice at 6 weeks of age, weighing 28–30 g, with normal estrus cycles, were purchased from the Lanzhou Veterinary Research Institute (License: Lanzhou Veterinary Research Institute SCXk2020-0002). Housing conditions: room temperature 20–26°C, indoor humidity 55–70%.

2.1.2. Drugs and reagents

Melatonin powder and cyclophosphamide powder were purchased from Shanghai Macklin Biochemical Technology Co., Ltd., with catalog numbers M813985-25g and C849559-500mg, respectively; 4% paraformaldehyde; hematoxylin and eosin (H&E) staining solution from Feijing Biotechnology Co., Ltd.; malondialdehyde (MDA), superoxide dismutase (SOD), glutathione peroxidase (GSH-PX) detection kits from Nanjing Jiancheng Bioengineering Institute; estradiol (E2), FSH, LH ELISA kits from Shanghai Enzyme-linked Biotechnology Co., Ltd.; protein extraction reagent and BCA protein concentration determination kit from Xin Sai Mei Biotechnology Co., Ltd.; p21 rabbit monoclonal antibody from Abcam; γH2AX mouse monoclonal antibody

(catalog number: JBW301) from Shanghai Baili Biotechnology Co., Ltd.; p53 rabbit polyclonal antibody and GAPDH rabbit antibody from Jiangsu Qinke Biotechnology Research Center Co., Ltd.; horseradish peroxidase-labeled goat anti-rabbit and goat anti-mouse secondary antibodies from Hangzhou Hua'an Biotechnology Co., Ltd.; 5× protein loading buffer (containing DTT) from Solaibo Company; universal antibody diluent from Suzhou Xin Sai Mei Biotechnology Co., Ltd.

2.1.3. Main instruments

The instruments included multi-functional full-wavelength microplate reader from Meigu Molecular Instruments (Shanghai) Co., Ltd.; Amersham Imager 600 electrophoresis imaging analysis system from GE Healthcare Bio-Sciences AB; incubator from Jintan Tianjing Experimental Instrument Factory; HWS-12 electric constant temperature water bath from Zhejiang Nade Scientific Instrument Co., Ltd.; German sigma high-speed frozen centrifuge 3k15 from Shanghai Lingyi Biotechnology Co., Ltd.; AX224ZH electronic balance from Ohaus Instrument Co., Ltd.; small electrophoresis instrument from Xi'an Tengling Biotechnology Co., Ltd.

2.2. Experimental methods

2.2.1. Animal grouping, modeling, and drug administration

Adaptive feeding for 5-week-old female Kunming mice for one week was followed by selecting mice with stable estrus cycles for subsequent experiments. The mice were randomly assigned to seven groups, with 20 mice per group: Normal group (Group A): No intervention; Blank control group (Group B): Intraperitoneal injection and gavage of normal saline; MT administration group (Group C): MT (15 mg/kg) gavage; CTX-induced POF model group (Group D): First-day intraperitoneal injection of 50 mg/kg CTX + continuous 14-day intraperitoneal injection of 8 mg/kg CTX [15]; Synchronous combined protection group: Low-dose Group E: Group D CTX dose + MT (7.5 mg/kg) gavage, Medium-dose Group F: Group D CTX dose + MT (15 mg/kg) gavage, High-dose Group G: Group D CTX dose + MT (30 mg/kg) gavage; MT was administered by gavage every day at 20:00 for 14 consecutive days [16].

2.2.2. Growth status and body mass changes

Following the modeling, mice in each group were observed and recorded during drug administration and feeding in order to observe their feeding, fur, and activity. At the same time, the body mass changes of the mice were monitored every other day and recorded, and the drug dosage was adjusted according to the body mass.

2.2.3. Changes in the estrus cycle

Every morning at 8 am, vaginal exfoliated cell detection was performed on mice in each group. The specific operation method is as follows: The mouse was held steady with one hand, while a pipette was held with the other to draw 200 μL of normal saline solution. The pipette was gently inserted into the mouse's vagina, and the saline solution was injected, followed by repeated rinsing 2 to 3 times. The rinsed solution was then aspirated and spread onto a pre-numbered slide. After settling and fixation, H&E staining was performed. The estrous cycle was determined using an optical microscope, recorded, and represented in a line chart. The normal estrus cycle of mice is stable for 4 to 5 days. When there is a prolongation of diestrus, continuous diestrus, or the estrus cycle of the mice becomes chaotic and lasts for more than 6 days, or there is a long-term stagnation in a certain period, it is considered that the mice have estrus cycle disorders and ovarian damage [17]. Microscopic observation

showing dominant flaky anuclear keratinized epithelial cells indicates estrus; when nuclear oval epithelial cells are dominant, it is proestrus; when a large number of white blood cells are dominant, it is diestrus; when all three types of cells exist, it is metestrus [18].

2.2.4. Changes in ovarian size and wet weight

After the modeling was completed, the mouse's whiskers were cut off, blood was taken from the eyeballs, and then the mouse was euthanized. The ovarian tissue was taken out, fat tissue was removed, and the ovarian length and wet weight were measured and recorded.

2.2.5. Changes in the pathological morphology of ovarian tissue

After soaking the ovarian tissue in 4% paraformaldehyde solution, it was inserted into paraffin, sectioned, and stained with H&E. The ovarian tissue morphology was observed under a light microscope, and the number of follicles at each stage was counted. The ratio of atretic follicles to total follicles (proportion of atretic follicles) was calculated. Microscopic follicle evaluation: Primordial follicles are defined as oocytes surrounded by a layer of squamous granulosa cells; primary follicles have oocytes surrounded by a layer of cubic granulosa cells; secondary follicles are surrounded by more than one layer of cubic granulosa cells, and follicular cavity has not yet formed; early antral follicles begin to develop a follicular cavity, and preovulatory antral follicles show distinct layered granulosa cell layers; atretic follicles have oocytes that are shrinking and irregularly shaped, with deeply stained zona pellucida [19].

2.2.6. Detection of serum hormones

Blood was collected from the eyeball and placed in a 1.5 ml EP tube, permitted to stratify at 4℃ in a refrigerator, and then centrifuged at 3500r/min for 10 minutes at 4℃ in a low-temperature centrifuge. The ELISA method was utilized to detect serum levels of FSH, E2, and LH, strictly adhering to the guidelines provided by the ELISA kit. The remaining serum was stored in a -80℃ freezer for future use.

2.2.7. Measurement of serum MDA, SOD, and GSH-PX

Frozen serum samples were thawed and used according to the antioxidant kit's instructions to measure the levels of MDA, SOD, and GSH-PX in mouse serum.

2.2.8. Western blot detection of related pathway protein expression

Ovaries stored at -80℃ were removed and crushed, and proteins were extracted. After detecting protein concentration using a BCA kit, 5× loading buffer was added according to the volume, boiled in water for 10 minutes, and then stored at -20℃ for future use. Equal amounts of protein were electrophoresed on a 6% or 10% SDS polyacrylamide gel. The gel was run at 80V until it exited the stacking gel (approximately 30 minutes), then at 100V until the end of the resolving gel (approximately 2 hours). A 5.5 cm × 8 cm PVDF membrane was cut, and a sandwich layer was made in the order of the black board, sponge pad, filter paper, gel, PVDF membrane, filter paper, sponge pad, and white board. The membrane was transferred at 120 mA for 2.5 hours. After transfer, the membrane was washed three times with 1× TBST for 10 minutes each, and then blocked with 5% BSA for one hour. The membrane was cut and incubated with primary antibodies p53 (1:1000), p21 (1:800), γH2AX (1:1000), and GAPDH (1:4000) at 4℃ overnight. Following the conclusion of the incubation phase, the membrane was

subjected to three washes with 1× TBST, each wash lasting for a period of 10 minutes. Subsequent to the removal of the primary antibody, the membrane was placed into a chamber containing HRP-conjugated goat anti-rabbit and goat anti-mouse secondary antibodies, where it remained for a duration of one hour at ambient temperature. Protein blots were visualized with enhanced luminescent reagent, and protein gray values were analyzed using ImageJ software. The expression levels of other proteins were calculated using GAPDH as an internal reference.

2.2.9. Statistical methods

The measured data obtained was statistically analyzed using Graph Pad Prism 10.1 software. Each experiment was repeated three times. Multiple groups were compared using one-way ANOVA, and further comparisons between two groups were performed using a *t*-test. A P-value < 0.05 was considered statistically significant.

3. Results

3.1. Effects of MT on the general condition of CTX-induced POF mice

Mice in the normal group and the blank control group had smooth hair, a good mental state, normal activity, and normal weight gain. Compared with the control group, the model group had sparse hair, rough and dull skin, significantly reduced activity, and lower body weight. Mice in the MT-only administration group and the low, medium, and high MT dose groups exhibited shiny hair and varying degrees of weight gain compared to the model group; however, these differences were not statistically significant (see **Figure 1**).

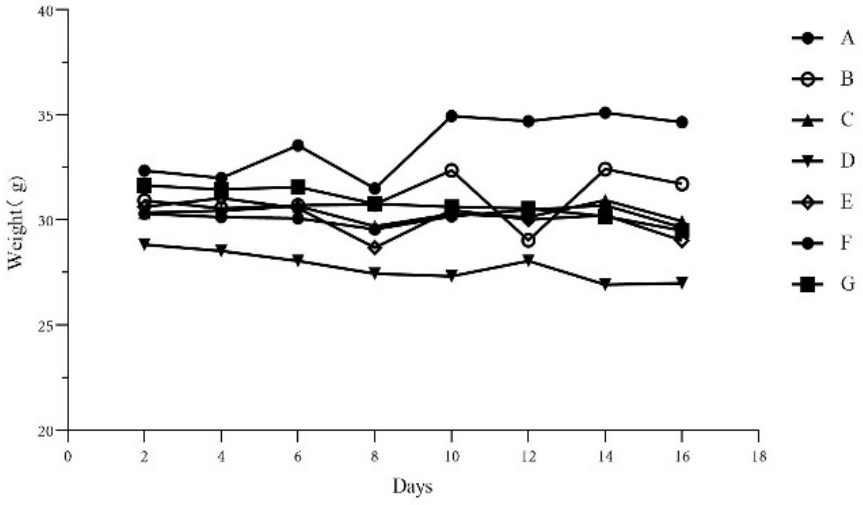

Figure 1. Line graph of changes in body weight of mice in each group. Note: Group A: Normal group, Group B: Control group, Group C: MT only group, Group D: Premature ovarian failure model group, Group E: Low-dose MT group, Group F: Medium-dose MT group, Group G: High-dose MT group.

3.2. The effect of MT on the estrus cycle of CTX-induced POF mice

The H&E staining results of vaginal exfoliated cells from mice are illustrated in **Figure 2**. After modeling, the estrus cycles of mice in the normal group, blank control group, and MT-only administration group were normal, averaging 4–5 days per cycle. However, in comparison to the blank control group, the premature ovarian failure model group exhibited disordered estrus cycles and varying degrees of estrus cycle prolongation, averaging 7–9

days per cycle, and some mice did not show a complete estrus cycle. After MT protection was administered, the estrus cycles of mice in each group showed varying degrees of recovery, with estrus cycles ranging from 5–7 days per cycle, which was shorter and more stable compared to the premature ovarian failure model group.

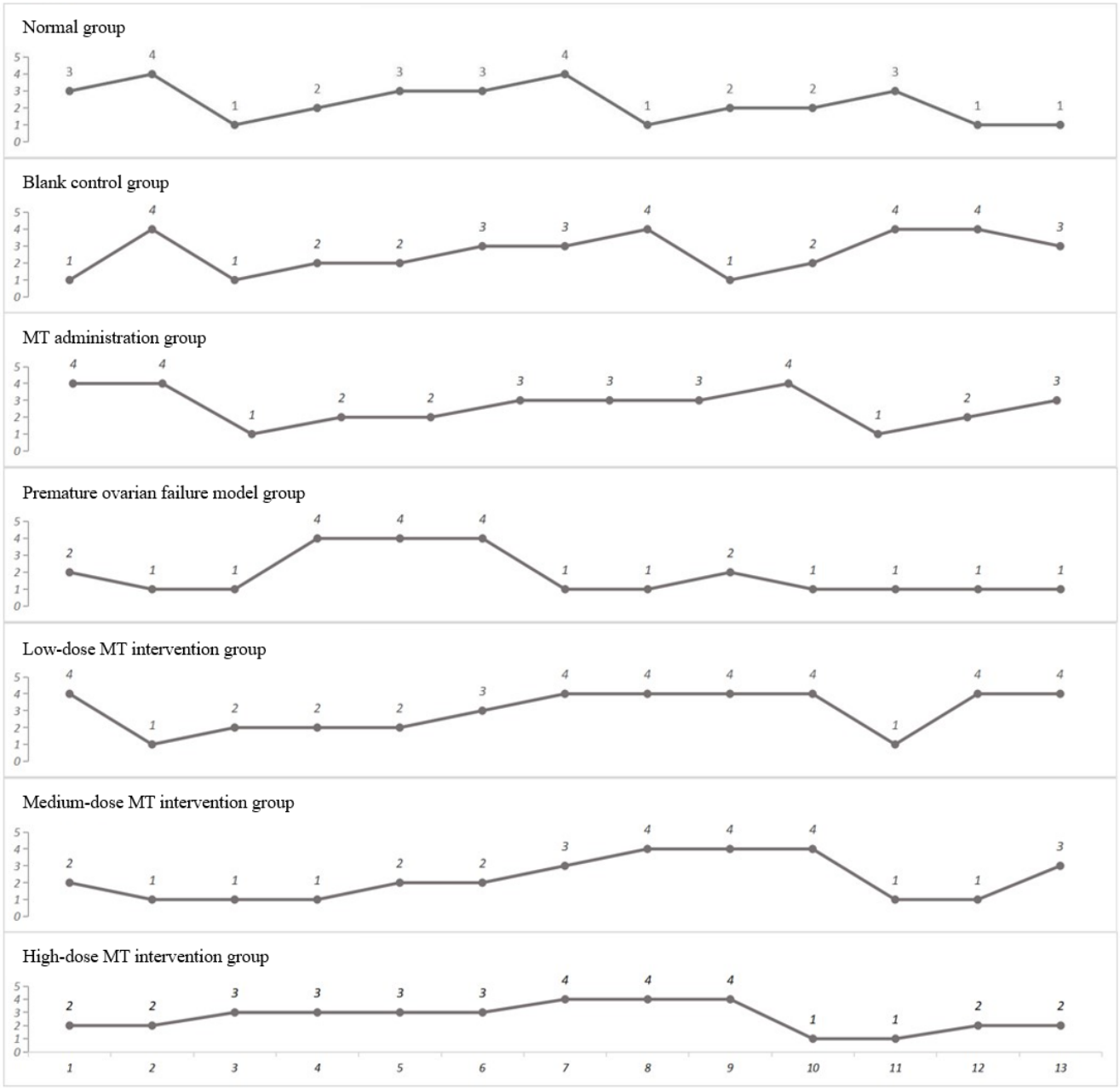

Figure 2. Line graph of the motility cycle during treatment in mice. Note: 1: Proestrus, 2: Estrus, 3: Metestrus, 4: Diestrus.

3.3. The effect of MT on ovary size and wet weight in CTX-induced POF mice

In the absence of statistical differences between the normal group and the blank control group, compared to the blank group, the ovarian diameter of mice in the model group was slightly reduced, but the difference was not statistically significant ($P > 0.05$). However, the ovarian wet weight of mice in the model group and the MT low, medium, and high dose groups were significantly reduced ($P < 0.01$, $P < 0.05$). There were no statistically significant changes in ovarian diameter and wet weight in the MT-only administration group ($P > 0.05$). Compared

to the model group, the ovary size and wet weight of mice in the MT low, medium, and high dose groups showed varying degrees of increase, but the difference was not statistically significant ($P > 0.05$), as shown in **Figure 3**.

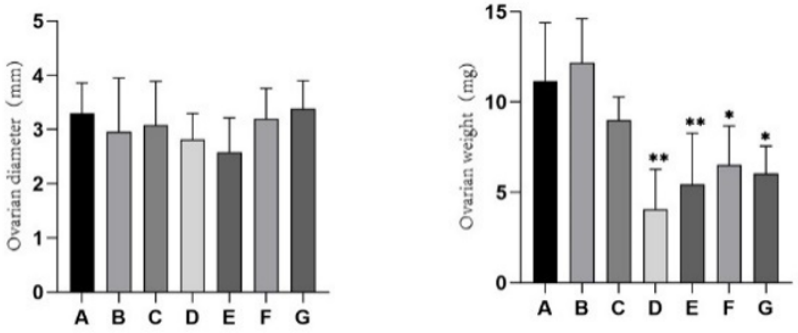

Figure 3. Comparison of ovary diameter and wet weight in each group of mice. Note: Compared with the control group: P < 0.05, *P < 0.01; compared with the premature ovarian failure model group: #P < 0.05, ##P < 0.01. Group A: Normal group, Group B: Control group, Group C: MT-only group, Group D: Premature ovarian failure model group, Group E: Low-dose MT group, Group F: Medium-dose MT group, Group G: High-dose MT group.

3.4. The effect of MT on the pathological morphology of ovarian tissue in CTX-induced POF mice

Statistical analysis of ovarian histopathological sections and follicle counts at various stages is shown in the figures. A large number of follicles and corpora lutea at various stages can be seen in the ovaries of mice in the normal group, control group, and MT-only administration group, with rare atretic follicles (see **Figure 4**). Compared to the control group, the number of primordial follicles, preantral follicles, and mature follicles in the model group mice was significantly reduced ($P < 0.05$, $P < 0.01$), while the number of atretic follicles was significantly increased compared to the control group ($P < 0.005$), with statistically significant differences. Compared to the model group, the number of primordial follicles, preantral follicles, and mature follicles in the ovaries of mice in the medium and high-dose MT treatment groups was significantly increased ($P < 0.05$, $P < 0.01$), and the number of atretic follicles was significantly reduced ($P < 0.005$, $P < 0.01$). However, compared to the control group, the changes in primordial follicles, preantral follicles, and mature follicles in the low-dose group were not significant, with only a noticeable reduction in the number of atretic follicles ($P < 0.05$).

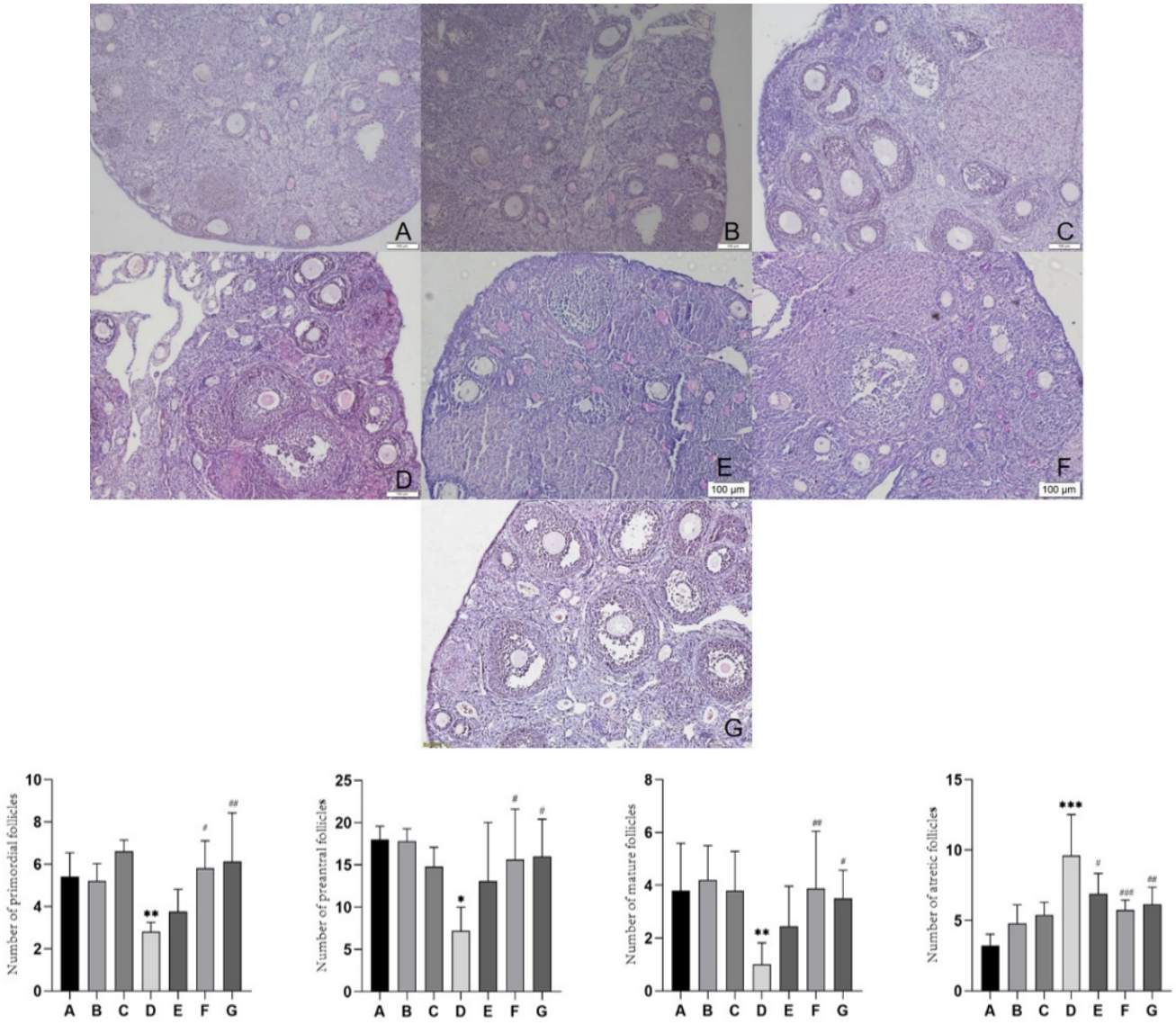

Figure 4. Morphological changes in ovarian tissue (H&E ×100) and follicle counts at all levels in all groups of mice. Note: Compared with the control group: $P < 0.05$, $P < 0.01$, $^{**}P < 0.005$; compared with the premature ovarian failure model group: $^{\#}P < 0.05$, $^{\#\#}P < 0.01$, $^{\#\#\#}P < 0.005$. Group A: Normal group, Group B: Control group, Group C: MT-only group, Group D: Premature ovarian failure model group, Group E: Low-dose MT group, Group F: Medium-dose MT group, Group G: High-dose MT group.

3.5. The effect of MT on serum hormones in CTX-induced POF mice

The levels of E2, FSH, and LH in the serum of mice in each group are shown in **Figure 5**. There were no statistically significant differences in the three hormone levels between the normal group and the blank control group ($P > 0.05$). Compared to the control group, the levels of LH and FSH in the serum of the model group were significantly increased ($P < 0.05$), while the level of E2 was significantly reduced ($P < 0.01$). Compared to the model group, the levels of LH and FSH in the serum of mice in the medium and high-dose MT groups were significantly reduced ($P < 0.05$), and the level of E2 was significantly increased ($P < 0.05$, $P < 0.01$). However, no statistically significant differences in hormone levels were observed between the low-dose MT group and the

model group ($P > 0.05$), suggesting that the observed effects may be related to the administered dose of MT.

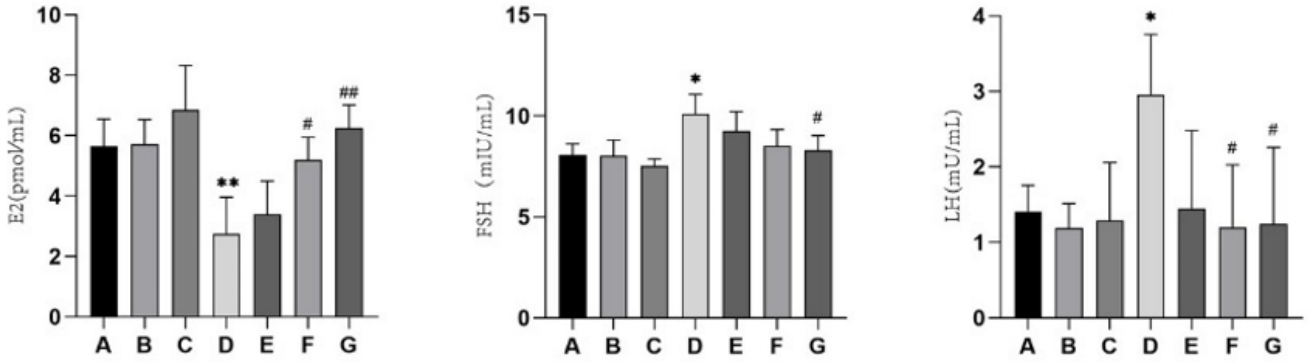

Figure 5. Comparison of serum E2, FSH, and LH in each group of mice. Note: Compared with the control group: $P < 0.05$, $^{*}P < 0.01$; compared with the premature ovarian failure model group: $^{\#}P < 0.05$, $^{\#\#}P < 0.01$. Group A: Normal group, Group B: Control group, Group C: MT-only group, Group D: Premature ovarian failure model group, Group E: Low-dose MT group, Group F: Medium-dose MT group, Group G: High-dose MT group.

3.6. The effect of MT on serum MDA, SOD, and GSH-PX levels in CTX-induced POF mice

As demonstrated in **Figure 6**, there were no statistically significant differences observed between the normal group and the blank control group, compared to the control group, the serum levels of SOD and GSH-PX in the model group were significantly reduced ($P < 0.05$, $P < 0.01$), while the MDA level was significantly increased ($P < 0.05$). Compared to the model group, the serum MDA level in the high-dose MT group was significantly reduced ($P < 0.005$), and the levels of SOD and GSH-PX were significantly increased ($P < 0.005$, $P < 0.01$). However, in the low-dose MT group, only the change in SOD level was significantly different from the model group ($P < 0.005$), and in the medium-dose MT group, only the change in MDA level was statistically significant compared to the model group ($P < 0.01$).

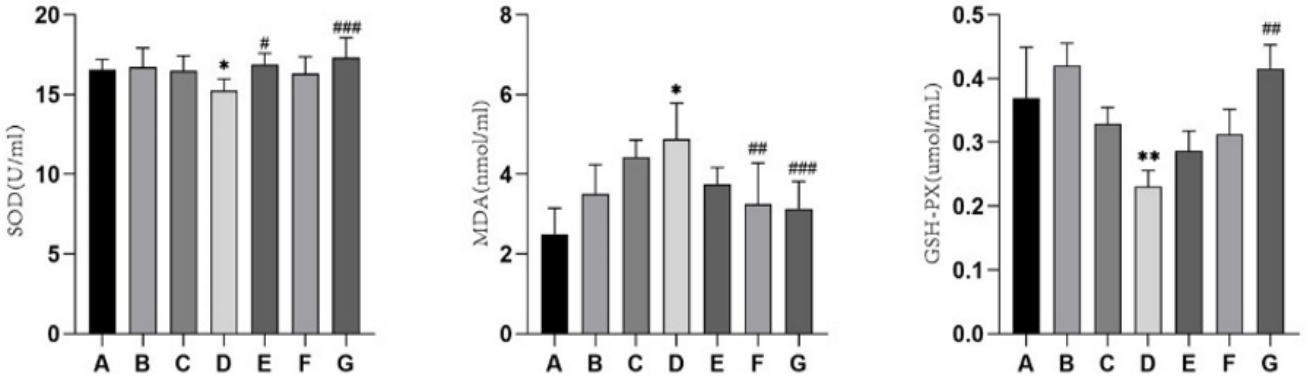

Figure 6. Comparison of MDA levels, SOD, and GSH-PX activities of mice in each group. Note: Compared with the control group: $P < 0.05$, $^{*}P < 0.01$; compared with the premature ovarian failure model group: $^{\#}P < 0.05$, $^{\#\#}P < 0.01$, $^{\#\#\#}P < 0.005$. Group A: Normal group, Group B: Control group, Group C: MT-only group, Group D: Premature ovarian failure model group, Group E: Low-dose MT group, Group F: Medium-dose MT group, Group G: High-dose MT group.

3.7. The effect of MT on the expression of DNA damage proteins in ovarian tissue of CTX-induced POF mice

Figure 7 illustrates the results of the Western blotting assay for the expression of DNA damage proteins in the ovaries of mice in each group. The bars indicate the comparison of grey values of the four protein bands under the premise that GAPDH was used as the internal reference. In comparison with the control group, the expression of DNA damage protein γH2AX was increased in the ovarian tissues of mice in the model group ($P < 0.05$), and the expression of p53 and p21 proteins was also significantly increased ($P < 0.01$). Conversely, the expression of γH2AX, p53, and p21 was found to be significantly downregulated in the ovaries of mice in the low-, medium-, and high-dose MT groups ($P < 0.05$, $P < 0.01$, $P < 0.005$, respectively). Among them, the changes in the expression of various proteins were most obvious in the high-dose group, and the differences were statistically significant.

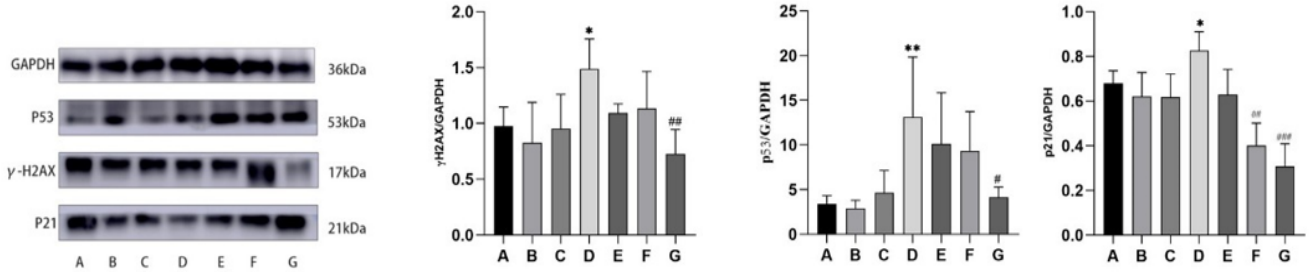

Figure 7. Comparison of the expression levels of DNA damage proteins in the ovarian tissues of mice in each group. Note: Compared with the control group: $P < 0.05$, $^{*}P < 0.01$; compared with the premature ovarian failure model group: $^{\#}P < 0.05$, $^{\#\#}P < 0.01$, $^{\#\#\#}P < 0.005$. Group A: Normal group, Group B: Control group, Group C: MT-only group, Group D: Premature ovarian failure model group, Group E: Low-dose MT group, Group F: Medium-dose MT group, Group G: High-dose MT group.

4. Discussion and conclusion

The global occurrence of POF is trending younger, and it poses varying degrees of harm to women's cardiovascular system, reproductive system, nervous system, and quality of life [20]. Due to the apparent trend of younger onset of tumors, POF caused by chemotherapy drugs has gradually received widespread attention. CTX, a commonly used antineoplastic drug in clinical practice, can produce two stable toxic compounds under the action of cytochrome P450: acrolein and phosphoramide nitrogen mustard. Acrolein has been demonstrated to induce the generation of reactive oxygen species (ROS) in a variety of cell lines within the body. An excessive accumulation of ROS within the organism has been shown to inhibit the activity of various enzymes within cells, instigate lipid peroxidation reactions, and result in DNA damage. In the female ovary, such an accumulation can precipitate accelerated follicular atresia and lead to premature depletion of the follicular pool, thus inducing ovarian failure [21-24]. Therefore, the use of antioxidants is of great significance to the female reproductive system, as it can effectively reduce the level of free radicals in the ovaries, thereby maintaining ovarian health and delaying female ovarian aging [25].

MT, as an antioxidant hormone that can be secreted by the human body itself, has been widely studied by scholars in recent years [26], and the positive effects of MT on the reproductive system have been documented. For example, Jones and Pepling found that MT promotes the quality of cumulus-oocyte complexes, facilitating

the development of primordial follicles to the next morphological stage [27]. Cruz *et al.* demonstrated that MT decreases the damage to proteins and DNA caused by oxidative stress by directly scavenging oxygen radicals and promoting glutathione synthesis [28]. According to Matikainen *et al.* [29], MT's ability to inhibit mitochondrial-mediated follicular apoptosis is attributed to its induction of Bcl2 in follicular granulosa cells and inhibition of caspase3 activity. Feng's [30] research shows that melatonin can affect macrophage polarization, regulate oxidative stress and chronic inflammation, and activate ovarian germline stem cells to delay chemotherapy-induced aging in mice. Additionally, MT can indirectly activate and stimulate antioxidant enzymes and inhibit pro-oxidant enzymes. It can also reduce oxidative damage to ovarian granulosa cells by inhibiting the JNK-BCL-2-BECN1 signaling pathway to inhibit autophagy [31].

In this study, we used CTX to construct a mouse model of POF and found that compared to the control group, the serum FSH and LH levels were elevated, while E2 levels were significantly reduced in the model group. Clinically, both LH and FSH are secreted by the pituitary gland and play a role in regulating sex hormone synthesis, promoting folliculogenesis, and corpus luteum formation [32]. E2 is a commonly used indicator for monitoring follicular growth and development in clinical practice. It can be used to evaluate ovarian reserve function. Most patients with ovarian failure clinically have estrogen deficiency, so a decrease in E2 levels may indicate insufficient ovarian reserve function [33]. The research conclusions of Melekoglu *et al.* [34] and Wei *et al.* [35] pointed out that compared with the control group, the mice in the model group had disordered estrus cycles and abnormal follicular development. The quantity of follicles at various developmental stages decreased, while the number of atretic follicles increased significantly. The disappearance of mature follicles suggests the successful establishment of a CTX-induced mouse model of POF, which is consistent with our research results [34,35]. In this study, serum FSH and LH levels were significantly lower and E2 levels were significantly higher in all groups of mice after co-protection with MT compared to the drug control group. These findings suggest that MT improves POF in mice. Changes in the estrus cycle and ovarian morphology of mice can reflect ovarian function and ovarian reserve [36,37]. After administering different doses of MT protection, the above conditions in mice were significantly improved, with the high-dose MT protection group showing the most significant improvement. This demonstrates that CTX is capable of inducing ovarian dysfunction and depletion of ovarian reserves in mice. Conversely, MT has been shown to restore ovarian function and preserve ovarian reserves to a certain extent, a finding that is in accordance with the research results reported by Jang *et al.* [38].

Clinically, MDA levels serve as a means of indicating the level of lipid peroxidation in the body and, indirectly, the level of cellular damage [39]. SOD and GSH-PX are key antioxidant molecules in the body. It has been proven that the ovaries can be shielded from oxidative stress harm by removing ROS and lipid peroxides [40]. The experimental study revealed that, in comparison with the control group, the serum level of the oxidative index MDA was elevated, while the levels of the antioxidant indexes SOD and GSH-PX were considerably reduced in the model group mice. However, these conditions were improved in the MT-protected mice, with the high-dose group showing the most significant effect. This suggests that CTX induces oxidative stress in mice, which MT can alleviate and improve. As a structurally stable non-enzymatic antioxidant, MT has a powerful antioxidant effect that scavenges hydroxyl radicals (·OH) and different ROS. In the body, the metabolites produced by the interaction between MT and free radicals are still powerful antioxidants. They can capture ROS through the 5-methoxy group on the indole ring, providing electrons to convert it into non-oxidizing substances, while converting itself into a low-toxicity intermediate N1-acetyl-N2-formyl-5-methoxykynurenamide. The latter has stronger antioxidant properties than MT and can scavenge a variety of ROS [41]. 6-hydroxy MT, formed after MT

metabolism in the liver, has an antioxidant capacity 30 times that of MT. It can protect the kidneys from oxidative stress damage induced by cisplatin drugs, counteract oxidative stress caused by cyanide, and inhibit Fe^{2+}-induced lipid peroxidation reactions. Through such antioxidant cascade reactions, it becomes a highly effective antioxidant [42]. Additionally, MT also has an indirect antioxidant effect. According to research by Pandi-Perumal *et al.*, MT can enhance GSH-PX activity in the liver, lungs, and brain of rats and increase the mRNA level of SOD in tissues [43].

Furthermore, this research aimed to explore the possible mechanism of MT's antioxidant protection against premature ovarian failure caused by CTX in mice. γH2AX is a clinically commonly used marker protein for DNA damage and is one of the earliest proteins to undergo changes at DSB sites. As a signaling molecule, γH2AX recruits other DNA repair proteins to the break site to initiate the repair mechanism [44,45]. Research has demonstrated that an excessive accumulation of ROS within the body can serve as a catalyst for the onset of oxidative stress, which, in turn, can precipitate DNA damage within human tissues [46]. The results of this study showed that the expression of γH2AX protein was significantly increased in the ovarian tissues of mice in the model group compared to the control group, suggesting that CTX induced DNA damage in mouse ovaries through oxidative stress. However, the expression of γH2AX protein in the ovarian tissues of mice in the MT-protected group was significantly reduced, thereby suggesting that MT alleviated DNA damage in mouse ovaries to a certain extent. The tumor suppressor p53 is the center of the DNA damage response and a key molecule that regulates apoptosis [47]. Liu *et al.* carried out a study that demonstrated a noteworthy increase in the mRNA and protein expression levels of p53 in the ovarian tissue of rats that were suffering from POF [48]. At the same time, as a transcription factor, there is a p53-centered signal transduction network in cells. The p53 protein has been demonstrated to regulate the expression of hundreds of downstream genes, thereby triggering a variety of biological processes, including the promotion of DNA repair, the induction of cell cycle arrest, and the promotion of cell senescence and apoptosis [49]. *P21* is a transcriptional target gene of p53 [50] and an inhibitor of the cyclin E-CDK2 complex. It can arrest the cell cycle in the G1 phase during the DNA damage response, preventing it from entering the S phase and blocking the cell cycle, thus allowing more time for damaged cells to repair [51]. Zhang's research showed that MT can slow down the phosphorylation level of p53 in busulfan-induced mouse spermatogonia through the ATM-p53 signaling pathway, thus avoiding the apoptosis of spermatogonial stem cells [52]. Studies have shown that melatonin can inhibit apoptosis by down-regulating pro-apoptotic genes such as *p53*, thereby improving the quality of mouse blastocysts [53]. Zhang showed that MT can down-regulate the expression of p53 and inhibit the transcription of its downstream genes by inhibiting oxidative stress, thereby rescuing bisphenol A-induced apoptosis and autophagy of mouse Leydig cells, and ultimately alleviating bisphenol A-induced damage to the male reproductive system in mice [54]. The results of Western Blot in this study suggested that compared with the control group. The expression levels of p53 and p21 proteins were found to be significantly higher in the ovarian tissues of the model group, whereas the expression levels of these two proteins were significantly lower in the ovarian tissues of the MT-protected groups. The changes in protein expression were most significant in the high-dose group. This indicates that the protective mechanism of MT against CTX-induced DNA damage in mouse ovaries may be related to γH2AX, p53, and p21. In summary, MT can improve estrous cycle disorders, abnormal follicular development, and changes in serum hormone levels caused by CTX-induced premature ovarian failure in mice, alleviate the occurrence of oxidative stress, and protect ovarian DNA from damage. It may exert antioxidant protection by affecting the expression of proteins such as γH2AX, p53, and p21. Although this study verified this hypothesis through animal experiments, further cell experiments are needed to explore the molecular mechanism and role of MT, which will be the focus of our next research.

Funding

2023 Special Project for Serving the National Development Strategy with Basic Scientific Research Fees from Central Universities (No. 31920230188); 2023 Northwestern Minzu University College-Level Innovation and Entrepreneurship Training Program (No. X202310742289); 2024 National College Students' Innovation and Entrepreneurship Training Program (No. 202410742005)

Disclosure statement

The authors declare no conflict of interest.

References

[1] Ruan X, Cheng J, Du J, et al., 2023, Application Value of Fertility Protection in the Prevention and Treatment of Premature Ovarian Insufficiency. Chinese Journal of Practical Gynecology and Obstetrics, 39(09): 913–917.

[2] Wu J, Yu Q, 2016, Diagnosis and Treatment of Premature Ovarian Insufficiency. Chinese Medical Information Herald, 31(21): 21.

[3] Podfigurna-Stopa A, Czyzyk A, Grymowicz M, et al., 2016, Premature Ovarian Insufficiency: The Context of Long-Term Effects. Journal of Endocrinological Investigation, 39(9): 983–990.

[4] Shelling ML, Kirsner RS, 2010, Failure to Counsel Patients with Psoriasis to Decrease Alcohol Consumption (and Smoking). Arch Dermatol, 146(12): 667–684.

[5] Wilson C 2011, Autoimmunity: Autoimmune Addison Disease and Premature Ovarian Failure. Nat Rev Endocrinol, 7(9): 498.

[6] Behret H, 1999, Assessment of Existing Chemicals: A Contribution Towards Improving Chemical Safety, Gesellschaft Deutscher Chemiker, Frankfurt am Main, Germany.

[7] Meskhi A, Seif MW, 2006, Premature Ovarian Failure. Current Opinion in Obstetrics & Gynecology, 18(04): 418–426.

[8] Spears N, Lopes F, Stefansdottir A, et al., 2019, Ovarian Damage from Chemotherapy and Current Approaches to its Protection. Human Reproduction Update, 25(06): 673–693.

[9] Zonta YR, Martinez M, Camargo ICC, et al., 2017, Melatonin Reduces Angiogenesis in Serous Papillary Ovarian Carcinoma of Ethanol-Preferring Rats International Journal of Molecular Sciences, 18(04): 763.

[10] Pascuali N, Scotti L, Di Pietro M, et al., 2018, Ceramide-1-Phosphate has Protective Properties against Cyclophosphamide-Induced Ovarian Damage in a Mice Model of Premature Ovarian Failure. Human Reproduction, 33(05): 844–859.

[11] Kovanci E, Schutt AK, 2015, Premature Ovarian Failure: Clinical Presentation and Treatment. Obstetrics and Gynecology Clinics of North America, 42(1): 153–161.

[12] Xing CH, Wang Y, Liu JC, et al., 2022, Melatonin Reverses Mitochondria Dysfunction and Oxidative Stress-Induced Apoptosis of Sudan I-Exposed Mouse Oocytes. Ecotoxicol Environ Saf, 225: 112783.

[13] He Q, Gu L, Lin Q, et al., 2020, The IMMP2L Mutation Causes Ovarian Aging Through ROS-Wnt/β-Catenin-Estrogen Pathway: Preventive Effects of Melatonin Endocrinology, (9): 9.

[14] Feng J, Ma WW, Li HX, et al., 2022, Melatonin Prevents Cyclophosphamide-Induced Primordial Follicle Loss by Inhibiting Ovarian Granulosa Cell Apoptosis and Maintaining AMH Expression. Frontiers in Endocrinology, 13: 895095.

[15] Fu X, He Z, 2008, Establishment of an Animal Model of Chemotherapy-Induced Premature Ovarian Failure. J Guangdong Medicine, (12): 1952–1954.

[16] Zhang L, Zhang X, Zhou J, et al., 2022, Effects of Melatonin and Follicle-Stimulating Hormone on Ovarian Follicle Development and Angiogenesis in Mice. Animal Husbandry and Veterinary, 54(05): 1–8.

[17] McLean AC, Valenzuela N, Fai S, et al., 2012, Performing Vaginal Lavage, Crystal Violet Staining, and Vaginal Cytological Evaluation for Mouse Estrous Cycle Staging Identification. Journal of Visualized Experiments: JoVE, (67): e4389.

[18] Zhu L, Luo S, Xu L, 2008, Study on Reproductive Capacity of Mice with Immune Premature Ovarian Failure. Chinese Medical Review, (06): 13–15.

[19] Zhang L, 2021, Effects and Mechanisms of Melatonin on Ovarian Follicle Development and Angiogenesis in Mice, thesis, Nanjing Agricultural University.

[20] Larsen EC, Muller J, Schmiegelow K, et al., 2003, Reduced Ovarian Function in Long-Term Survivors of Radiation- and Chemotherapy-Treated Childhood Cancer. The Journal of Clinical Endocrinology and Metabolism, 88(11): 5307–5314.

[21] Sanchez-Barcelo EJ, Mediavilla MD, Alonso-Gonzalez C, et al., 2012, Melatonin Uses in Oncology: Breast Cancer Prevention and Reduction of the Side Effects of Chemotherapy and Radiation. Expert Opinion on Investigational Drugs, 21(6): 819–831.

[22] Vaupel P, Mayer A, 2007, Hypoxia in Cancer: Significance and Impact on Clinical Outcomes. Cancer Metastasis Reviews, 26(2): 225–239.

[23] Talib WH, Saleh S, 2015, Propionibacterium acnes Augments Antitumor, Anti-Angiogenesis and Immunomodulatory Effects of Melatonin on Breast Cancer Implanted in Mice. PLoS One, 10(4): e0124384.

[24] Desmeules P, Devine PJ, 2006, Characterizing the Ovotoxicity of Cyclophosphamide Metabolites on Cultured Mouse Ovaries. Toxicological Sciences: An Official Journal of the Society of Toxicology, 90(2): 500–509.

[25] Wang S, He G, Chen M, et al., 2017, The Role of Antioxidant Enzymes in the Ovaries. Oxidative Medicine and Cellular Longevity, 2017: 4371714.

[26] Aversa S, Pellegrino S, Barberi I, et al., Potential Utility of Melatonin as an Antioxidant During Pregnancy and in the Perinatal Period. J Matern Fetal Neonatal Med, 25(3): 207–221.

[27] Jones RL, Pepling ME, 2013, Role of the Antiapoptotic Proteins BCL2 and MCL1 in the Neonatal Mouse Ovary. Biology of Reproduction: Offical Journal of the Society for the Study of Reproduction, 88(2): 46.

[28] Cruz MH, Leal CL, Cruz JF, et al., 2014, Essential Actions of Melatonin in Protecting the Ovaries from Oxidative Damage. Theriogenology, 82(7): 925–932.

[29] Matikainen T, Perez GI, Zheng TS, et al., 2001, Caspase-3 Gene Knockout Defines Cell Lineage Specificity for Programmed Cell Death Signaling in the Ovary. Endocrinology, 142(6): 2468–2480.

[30] Feng J, 2022, The Role of Melatonin in Delaying Chemotherapy-Induced Ovarian Aging through Antioxidant, thesis, Nanchang University.

[31] Alamro A, Al-Malky M, Ansari MGA, et al., 2022, The Effects of Melatonin and Vitamin D3 on the Gene Expression of BCl-2 and BAX in MCF-7 Breast Cancer Cell Line. Journal of King Saud University–Science, 33(2): 101287.

[32] Fortune JE, 1994, Ovarian Follicular Growth and Development in Mammals. Biology of Reproduction, 50(2): 225–232.

[33] Xu L, Song Y, 2003, Clinical Manifestations and Diagnostic Criteria of Premature Ovarian Failure. Journal of Practical Obstetrics and Gynecology, (04): 195–196.

[34] Melekoglu R, Ciftci O, Eraslan S, et al., 2018, Beneficial Effects of Curcumin and Capsaicin on Cyclophosphamide-Induced Premature Ovarian Failure in a Rat Model. J Ovarian Res, 11(1): 33.

[35] Wei T, Ling L, Feng X, et al., 2018, Effects and Mechanisms of Cyclophosphamide on the Structure and Function of Rat Ovaries. Journal of PLA Medical Journal, 43(03): 195–200.

[36] Zhu N, Jia H, Liu X, et al., 2012, Developmental Dynamics of Mouse Follicles in Estrus Cycle and its Effect on Superovulation. Zoological Study, 33(03): 276–282.

[37] Sun H, Wang F, Zhang P, et al., 2005, Research Progress in Monitoring Ovarian Reserve Function and Prediction of Premature Ovarian Failure. Foreign Medicine (Family Planning Volume), (05): 43–47.

[38] Jang H, Lee OH, Lee Y, et al., 2016, Melatonin Prevents Cisplatin-Induced Primordial Follicle Loss via Suppression of PTEN/AKT/FOXO3a Pathway Activation in the Mouse Ovary. Journal of Pineal Research, 60(3): 336–347.

[39] Zia A, Farkhondeh T, Pourbagher-Shahri AM, et al., 2021, The Role of Curcumin in Aging and Senescence: Molecular Mechanisms. Biomedicine & Pharmacotherapy, 134: 111119.

[40] Causer AJ, Shute JK, Cummings MH, et al., 2020, Circulating Biomarkers of Antioxidant Status and Oxidative Stress in People with Cystic Fibrosis: A Systematic Review and Meta-Analysis. Redox Biology, 32: 101436.

[41] Tan DX, Manchester LC, Terron MP, et al., 2007, One Molecule, Many Derivatives: A Never-Ending Interaction of Melatonin with Reactive Oxygen and Nitrogen Species? Journal of Pineal Research, 42(1): 28–42.

[42] Srinivasan V, Spence DW, Pandi-Perumal SR, et al., 2008, Therapeutic Actions of Melatonin in Cancer: Possible Mechanisms. Integrative Cancer Therapies, 7(3): 189–203.

[43] Pandi-Perumal SR, Bahammam AS, Brown GM, et al., 2013, Melatonin Antioxidative Defense: Therapeutical Implications for Aging and Neurodegenerative Processes. Neurotoxicity Research, 23(3): 267–300.

[44] D'Adda Di Fagagna F, Reaper PM, Clay-Farrace L, et al., 2003, A DNA Damage Checkpoint Response in Telomere-Initiated Senescence. Nature, 426(6963): 194–198.

[45] Smith SK, Kipling D, 2004, The Role of Replicative Senescence in Cancer and Human Ageing: Utility (or Otherwise) of Murine Models. Cytogenetics and Genome Research, 105(2–4): 455–463.

[46] Ran M, Gao H, Yin J, et al., 2013, Oxidative Stress and DNA Damage. Journal of Animal Nutrition, 25(10): 2238–2245.

[47] Abuetabh Y, Wu HH, Chai C, et al., 2022, DNA Damage Response Revisited: The p53 Family and its Regulators Provide Endless Cancer Therapy Opportunities. Experimental & Molecular Medicine, 54(10): 1658–1669.

[48] Liu TE, Zhang L, Wang S, et al., 2015, Tripterygium Glycosides Induce Premature Ovarian Failure in Rats by Promoting p53 Phosphorylation and Activating the Serine/Threonine Kinase 11-p53-p21 Signaling Pathway. Experimental and Therapeutic Medicine, 10(1): 12–18.

[49] Li H, 2013, Kinetics of p53 Signal Transduction Network Response to DNA Damage, thesis, Nanjing University.

[50] El-Deiry WS, 1993, WAF1, a Potential Mediator of p53 Tumor Suppression. Cell, 75(4): 817–825.

[51] Waldman T, Kinzler KW, Vogelstein B, 1995, p21 Is Necessary for the p53-Mediated G1 Arrest in Human Cancer Cells. Cancer Res, 55(22): 5187–5190.

[52] Zhang X, 2018, Study on the Mechanism of Calcitonin CDH22 Regulating the Self-Renewal of Female Germ Stem Cells and the Application of Melatonin in Fertility Maintenance, Doctoral dissertation, Nanjing Agricultural University.

[53] Wang F, 2014, Mechanism of Resveratrol and Melatonin on Oocyte Maturation and Embryonic Development, Doctoral dissertation, China Agricultural University.

[54] Zhang M, 2024, Mechanism of Apoptosis and Autophagy Induced by Bisphenol A in Mouse Testicular Stromal Cells and the Protective Effect of Melatonin, dissertation, Nanchang University.

Publisher's note

Bio-Byword Scientific Publishing remains neutral with regard to jurisdictional claims in published maps and institutional affiliations.